AAPS PharmSciTech, Vol. 11, No. 4, December 2010 (© 2010)
DOI: 10.1208/s12249-010-9533-6

Research Article

Application of Modeling to Scale-up Dissolution in Pharmaceutical Manufacturing

Venkat Koganti,[1,4] Fred Carroll,[1] Richard Ferraina,[1] Rick Falk,[2] Yogesh Waghmare,[2] Mark Berry,[1] Yang Liu,[1] Kenneth Norris,[1] Robert Leasure,[3] and Jeffrey Gaudio[3]

Received 9 July 2010; accepted 13 October 2010; published online 28 October 2010

Abstract. Liquid mixing scale-up in pharmaceutical industry has often been based on empirical approach in spite of tremendous understanding of liquid mixing scale-up in engineering fields. In this work, we attempt to provide a model-based approach to scale-up dissolution process from a 2 l lab-scale vessel to a 4,000 l scale vessel used in manufacturing. Propylparaben was used as a model compound to verify the model predictions for operating conditions at commercial scale that would result in similar dissolution profile as observed in lab scale. Geometric similarity was maintained between both of the scales to ensure similar mixing characteristics. We utilized computational fluid dynamics (CFD) to ensure that the operating conditions at laboratory and commercial scale will result in similar power per unit volume (P/V). Utilizing this simple scale-up criterion of similar P/V across different scales, results obtained indicate fairly good reproducibility of the dissolution profiles between the two scales. Utilization of concepts of design of experiments enabled summarizing scale-up results in statistically meaningful parameters, for example −90% dissolution in lab scale at a given time under certain operating conditions will result in 75–88% at commercial scale with 95% confidence interval when P/V is maintained constant across the two scales. In this work, we have successfully demonstrated that scale-up of solid dissolution can be done using a systematic process of lab-scale experiments followed by simple CFD modeling to predict commercial-scale experimental conditions.

KEY WORDS: CFD; dissolution; scale-up; tank mixing.

INTRODUCTION

Liquid mixing is a commonly used unit operation in pharmaceutical manufacturing to produce liquid dosage forms (*e.g.*, injectable solutions, oral solutions, oral suspensions, *etc.*). Scale-up of liquid mixing operations is far from being a linear exercise in which a process developed in lab scale (typically in a beaker using a stir bar) is scaled up to a manufacturing vessel. Selection of the manufacturing vessel is typically based on which mixing vessel is available and prior experience with a particular set of operating conditions in a vessel. Although above are often common practices to manufacture large-scale batches, they tend to overlook some basic questions such as – which aspects of the liquid mixing operation could fail during scale-up; will all of the solids be dissolved in a reasonable or targeted time frame; will there be foaming at large scale that will impact manufacturing; what is the impact of the geometry of the tank; what is the appropriate mixing equipment (impeller and vessel); are there critical attributes and how can they be understood and controlled; and how will the operating conditions during mixing (mixing speed, temperature of operation, *etc.*) affect the unit operation.

A well-designed scale-up operation would consider all of the above issues prior to scaling up a liquid mixing operation. Potential scale-up issues should be identified for risk analysis and design of appropriate experiments to understand and mitigate. One key factor that should be understood is the effect of tank geometry on scale-up. Once a tank and suitable paired mixing equipment is chosen, operating conditions should be defined. Ideally, this can be accomplished with mathematical models to predict operating conditions at commercial scale coupled with a combination of well-planned

[1] Pfizer Global Research and Development, Pfizer Inc, 558 Eastern Point Rd, Groton, Connecticut 06340, USA.
[2] Bend Research Inc., Bend, Oregon, USA.
[3] Pfizer Global Manufacturing, Pfizer Inc., Kalamazoo, Michigan, USA.
[4] To whom correspondence should be addressed. (e-mail: venkat.koganti@pfizer.com)

NOMENCLATURE: a, Interfacial area (m^2/m^3); k, Interface solid–liquid mass transfer coefficient; C, Concentration of dissolved solid in bulk liquid (mol/m3); C^*, Concentration of dissolved solid at the interface (mol/m3); D, Impeller diameter (m); N_D, Molecular diffusivity (m^2/s); K, Mass transfer coefficient (m/s); Re_p, Particle Reynolds number $(= \rho_f \varepsilon^{1/3} d_p^{4/3} / \mu_f)$; Sc, Schmidt number $(=\vartheta/D)$; Sh, Sherwood number $(=k\ d_p/D)$; T, Tank diameter (m); u_t, Terminal settling velocity of particle (m/s); N, Impeller speed (rev/s); N_{SG}, Minimum impeller speed for complete suspension of the particles; ρ_f, Fluid density (kg/m^3); ε, Turbulent dissipation rate (m^2/s^3); μ_f, Absolute viscosity (N.m/s); ϑ, Kinematic viscosity (m^2/s).

lab-scale experiments that would target a similar performance at commercial scale as observed at lab scale.

In this work, we utilize the above mentioned approach to scale-up of solid dissolution processing from lab-scale equipment to commercial-scale equipment. As mentioned previously solid dissolution is a common process unit operation during liquid mixing in the pharmaceutical industry. Incomplete dissolution can result in sub-potent batches resulting in batch failure. Competing elements such as the time required for dissolution *versus* the potential of microbial contamination over an extended mixing period may also be in play in a manufacturing setting.

A key fluid dynamic parameter that will govern the dissolution time is the solid/liquid mass transfer coefficient. We can define the mass transfer coefficient as the rate of mass transferred per unit time, per unit interface area, per unit concentration difference across the bulk phase and the interface. In other words,

$$\text{Rate of mass transfer} = k\,a(C^* - C) \tag{1}$$

where k is the solid–liquid mass transfer coefficient, a is interfacial area, C^* is the concentration at the interface that is saturation concentration, and C is the concentration in the bulk liquid phase. Thus by definition, achieving a constant mass transfer coefficient across different scales one should achieve similar dissolution rates and hence similar dissolution times, when all other parameters (interface area for mass transfer and concentration gradient) are held constant.

In order to achieve constant mass transfer coefficients across different scales; it is important to know how the mass transfer coefficient is affected by different operating parameters. Several correlations have been reported in literature. Brian *et al.* originally proposed the following functional relationship of the form based on Kolmogorov theory (1).

$$\mathrm{Sh} = f\left[\frac{\varepsilon d_\mathrm{p}^4}{\vartheta}; \mathrm{Sc}\right] \tag{2}$$

where Sherwood number $\mathrm{Sh}=k\ d_\mathrm{p}/N_\mathrm{D}$, d_p is diameter of particle in meter (m) and N_D is molecular diffusivity in m^2/s. Schmidt number $\mathrm{Sc}=\vartheta/N_\mathrm{D}$ where ϑ is kinematic viscosity in m^2/s. ε is turbulent energy dissipation rate in m^2/s^3. This functional form was further developed by Levins and Glastonbury who proposed (2,3)

$$\mathrm{Sh} = 2 + 0.47\,\mathrm{Re}_\mathrm{P}^{0.62}\,\mathrm{Sc}^{0.36}\left(\frac{D}{T}\right)^{0.17} \tag{3}$$

where particle Reynolds number Re_p is defined as

$$\mathrm{Re}_\mathrm{p} = \frac{\rho_\mathrm{f}\varepsilon^{1/3}d_\mathrm{P}^{4/3}}{\mu_\mathrm{f}} \tag{4}$$

where ρ_f and μ_f are fluid density and viscosity, respectively. The turbulent dissipation rate term, ε, can easily be replaced with power per unit volume (P/V) for stirred tank assuming all the power input is dissipated in the form of turbulence. This correlation seems to be widely accepted in the engineering community (4,5).

For particles with high density differences, the following correlation was proposed by Levins and Glastonbury (3)

$$\mathrm{Sh} = 2 + 0.44\,\mathrm{Re}_\mathrm{P}^{0.5}\,\mathrm{Sc}^{0.38} \tag{5}$$

Where Reynolds number is based on terminal settling velocity μ_t of particle

$$\mathrm{Re}_\mathrm{p} = \frac{\rho_\mathrm{f}u_\mathrm{t}d_\mathrm{p}}{\mu_\mathrm{f}} \tag{6}$$

Recently, Pangarkar *et al.* used a different approach and proved that the mass transfer coefficient can be correlated to relative particle suspension speed (6).

$$k = 5.31\times10^{-5}\left(\frac{N}{N_\mathrm{SG}}\right) \tag{7}$$

where N_SG is the minimum impeller speed for complete suspension of the particles and N is the impeller speed. Levins and Glastonbury pointed out that the correlations based on dissipation rate are strictly valid only if local dissipation rates are used (3). In a typical stirred tank, order of magnitude variation in local dissipation rate occurs. Okamoto *et al.* reported a 50 fold variation in dissipation rate from the impeller region to the near wall region (4). This distribution of energy is one possible reason behind variation in mass transfer coefficient for different impeller designs and tank geometries. This emphasizes the importance of keeping geometric similarity across different scales.

Although a vast volume of literature focuses on scale-up of solid–liquid mixing processes based on the criteria of complete solid suspension, systematic scale-up studies based on the criteria of equal mass transfer coefficients (or equal dissolution times) are rare. The use of constant power unit volume as a tentative scale-up rule is recommended in Perry's Handbook with a caution note to maintain the geometric similarity and the need for experimental validation (7). A scale-up by constant impeller speed was indicated by Barker and Treybal (8). Work by Hughmark suggests that mass transfer scale-up should be the same as particle suspension scale-up where P/V α $D^{-0.55}$ (9). Systematic analysis presented by Levins and Glastonbury suggests use of the P/V rule for geometrically similar vessels when the density difference between solid and liquid is small (3). In other words, P/V criteria should be used when the tank is operated at a higher agitation rate than that is needed for just suspension of the solids. In cases where the density difference is higher or the tank is operated near or below the just suspension speed, scale-up should be done based on equal tip speed.

In this work, the applicability of the following scale-up principle is considered when scaling up a solid dissolution process: When similar P/V is maintained across two different scales, it results in similar solid–liquid mass transfer coefficient when the two scales are geometrically similar to each other. We investigate the above noted principles of liquid mixing scale-up of the solid dissolution process. The objective is to demonstrate that using simple, single phase simulations coupled with systematic lab-scale experiments in geometrically similar equipment, we can predict operating conditions at commercial scale. In these evaluations, Propylparaben is used as a model compound. Design of experiments (DoE)

approach has been used to design the experiments at lab and commercial scale. This has provided for statistical predictions of dissolution time at commercial scale based on lab-scale experiments. This work paves the way for a rational scale-up approach for liquid mixing processes that is targeted to be the standard in the spirit of quality by design guidelines that pharmaceutical manufacturing continues to strive toward.(10)

EXPERIMENTAL METHODS

Computational Fluid Dynamics Simulations

Computational fluid dynamics (CFD) modeling was utilized to predict the mixing speeds at lab scale that would result in similar P/V compared with commercial scale for corresponding mixing. Tank geometries were generated and meshed using Gambit 2.4.6. supplied by ANSYS Inc. The number of cells used were approximately 600,000 which include hexahedral and tetrahedral elements. A grid independence study was not performed for this work but it is a standard practice to use few hundred thousand grid elements to model industrial scale tanks (11). CFD simulations were performed using a commercial software package Fluent 6.3.26. supplied by ANSYS Inc. All the cases were modeled as single phase, steady state with multiple reference frame. Standard k-ε turbulence model was used for all the cases. Second-order upwind discretization scheme and SIMPLE velocity-pressure coupling was used. It was assumed that the distortion of the free surface is negligible in terms of its effect on the velocities elsewhere in the tank. The curvature of the free surface was visually inspected and this assumption was confirmed. Following this assumption free surface was treated as a symmetry boundary condition. No slip boundary condition was used for the tank wall, impeller, shaft and baffles. Simulations were run until the force on the impeller and the flow rate through the impeller reached steady state. It was made sure that the residues were below 10^{-3} at the end of the simulation. Simulations required up to 3 days of computation time on four processors.

Converged flow field was used to calculate power input according to Paul *et al.* (5):

$$\frac{P}{V} = \frac{2\pi N \tau}{V} \tag{8}$$

Where N is stirrer speed in (revolutions per second (rps) and τ is the torque (N.m) acting on the impeller obtained from CFD model. It has been shown that RANS-based CFD simulations of stirred tanks using two-equation turbulence models can under-predict quantities such as turbulence kinetic energy and dissipation rate (12). However, it has also been shown that these types of simulations can predict flow quantities such as mean fluid velocity and power consumption based on Eq. 6 with reasonable accuracy (13). Therefore, P/V was calculated from the CFD simulations from impeller torque rather than from the volume-averaged turbulence dissipation rate. Blend time/tracer simulations were performed by solving a species equation after a converged flow field had been obtained following the procedures of Jaworski *et al.* (14). The continuity, momentum, and turbulence scalar transport equations were frozen while the scalar transport equation was solved for a small amount of a tracer material introduced into the tank. Second-order discretization scheme was used for solving the species equation.

In this work we used a 2-l vessel for lab-scale experiments while commercial-scale runs were conducted in a 4,000-l tank that has a fixed impeller. The 2-l scale stirred tank and the corresponding impeller were designed to be geometrically similar to 4,000-l tank. Key aspect ratios were maintained constant across both of the scales. The key ratios were—impeller diameter/tank diameter, liquid height/tank diameter, distance between impeller/tank diameters (C/T). Figure 1 illustrates these key tank dimensions and Table I lists the absolute values of these ratios on both of the scales for direct comparison.

Lab and Commercial-Scale Experiments

As mentioned above propylparaben was used as a model compound. The material was sourced from Mallinckrodt Baker Inc and same material was used for both lab and commercial-scale experiments. Propylparaben was sieved using 18 mesh stainless sieve before adding to the mixing tank. Malvern Mastersizer 2000 was used to measure particle size (volume weighted mean diameter of 179 μm) and specific surface area (0.188 m^2/g) of the sieved material. After assuring the geometric similarity between the two scales, three mixing speeds were selected at the commercial scale to span a typical operating range of the impeller. In addition to the mixing speed range, three operating temperatures across a range were selected due to the nature of propylparaben manufacturing efficiency. As temperature increases saturation solubility of propylparaben increases thus increasing the driving force for mass transfer between solid and liquid phases. Utilizing a DoE type approach, ten experimental runs were conducted at commercial and lab-scale spanning the three mixing speeds and three operating temperatures. Water

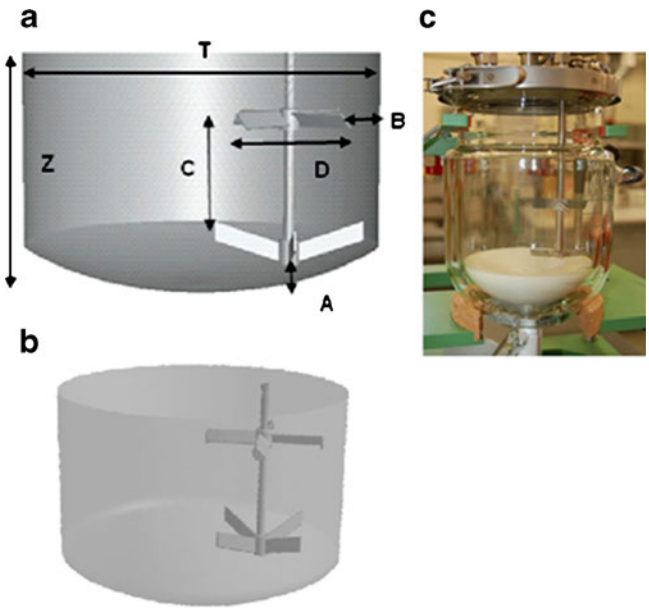

Fig. 1. Geometric details of tanks; **a** key dimensions, **b** schematic of 4,000-l tank, and **c** 2-l tank. The *white insert* in **c** is used to reduce the curvature of the lab-scale mixing tank thus making it similar to the commercial-scale tank

Table I. Summary of Operating Conditions at Commercial Scale and Lab Scale

	Commercial Scale	Lab Scale
Maximum rated capacity (l)	4,000	2
Batch size used in this study (l)	2,500	1.58
D/T	0.41	0.41
Z/T	3.47	3.14
C/T	0.4	0.4
A/T	0.04	0.03
B/T	0.06	0.05
Amount of propylparaben added to tank (g)	587	0.371
Final concentration of propylparaben upon complete dissolution (mg/ml)	0.235	0.235

D/T impeller diameter/tank diameter, *Z/T* fill height/tank diameter, *C/T* distance between impellers/tank diameter, *A/T* clearance from tank bottom to impeller bottom/tank diameter, *B/T* distance between side wall and impeller/tank diameter

was used as the solvent. Details of the experiments are shown in Table II. Saturation solubility of propylparaben at the three operating temperatures is listed in Table III. These values are calculated based on the non-linear van't Hoff solubility-temperature plots reported by Grant *et al*. (15). The quantity of propylparaben added at both the scales was selected so that it would result in same final concentration upon complete dissolution at both the scales. This concentration was based on the formulation concentration of propylparaben in an ongoing development project. The solubility data listed in Table III suggests that the final concentration in the tank (0.235 mg/ml) is much less than the saturation solubility at all three operating temperatures. We can therefore assume sink conditions in all of the experimental runs. Complete details of quantities of materials, batch sizes, and concentrations are also mentioned in Table I. The small scale experiments at lab scale were followed by large-scale experimental runs at commercial scale. After completion of each experiment, the solution was filtered through syringe filters and the filtrate was assayed by high-pressure liquid chromatography (HPLC) to confirm the paraben concentration.

Table II. Summary of Experimental Runs Conducted at Lab and Commercial-Scale Runs

Run ID	Mixing Speed at Lab Scale (rpm)	Mixing Speed at Commercial Scale (rpm)	Operating Temperature (°C)	P/V
1	210	45	45	87
2	290	60	45	206
3	360	75	45	402
4	210	45	55	87
5	290	60	55	206
6	290	60	55	206
7	360	75	55	402
8	210	45	65	87
9	290	60	65	206
10	360	75	65	402

This is factorial design with two center points (run ID #5 and 6)
P/V power per unit volume

Table III. Saturation Solubility of Propylparaben in Water at Three Operating Temperatures

Temperature (°C)	Solubility (mg/ml)
45	0.97
55	1.67
65	2.97

These numbers are calculated based on literature (15)

In lab-scale experiments the dissolution rate was monitored using Zeiss MCS 501 UV spectrometer that used a Helma transflectance dip probe with 1 mm path length. Spectra were collected every 10 s at 240 nm varied linearly as a function of propylparaben concentration during method validation. Hence intensity at 240 nm was monitored to monitor dissolution. A similar procedure was followed at commercial scale except that the path length of the UV probe used in large scale was 2 mm. This allowed for spectral acquisition every 10 s across a range of wavelengths during the dissolution of the propylparaben. The probe was located on the commercial tank at the apex of the tank wall and the bottom surface of the tank no more than 6" from the offset agitator blade. The lab-scale UV probe was located proportionally in the same proximity. Analysis of absorbance values at the appropriate wavelengths (240 nm in this study) provided a means of evaluating dissolution of the propylparaben over time in the commercial scale. This measurement set-up provided dissolution rate profiles of propylparaben for all the experimental runs that were conducted in the lab and at the commercial scale for comparison.

For the blend time studies, a pre-dissolved solution of methylparaben was added to the commercial tank and the concentration of methylparaben was monitored using UV/Vis spectra at the bottom of the tank. Three liters of pre-dissolved methylparaben solution at a concentration of 2.4 mg/ml was added to the tank containing 2,500 kg of water being mixed at a given speed. Three liters was sufficiently small enough for the entire aliquot to be added at once, thus simulating addition of tracer material as simulated in the CFD simulations. The concentration was chosen so that the final concentration in the tank is above the limit of quantitation of methylpraben. Even though propylparaben was used for the dissolution studies, the solubility of propylparaben was low enough that it required a large amount of pre-dissolved solution for the final concentration in the tank to be above limit of quantitation. This large volume cannot be added at once when compared with 3 l aliquot of methylparaben. The concentration profile from this experiment was compared with the blend time calculation obtained from CFD simulations where the concentration of the tracer was monitored

Table IV. Experimental Details of the Run to Find Blend Time

Scale of the Run	Commercial Scale
Batch size in the mixing tank prior to addition of concentrate (l)	2,500
Volume of concentrated methylparaben added (l)	3
Concentration of methylparaben in the concentrate that is added to the tank (mg/ml)	2.4

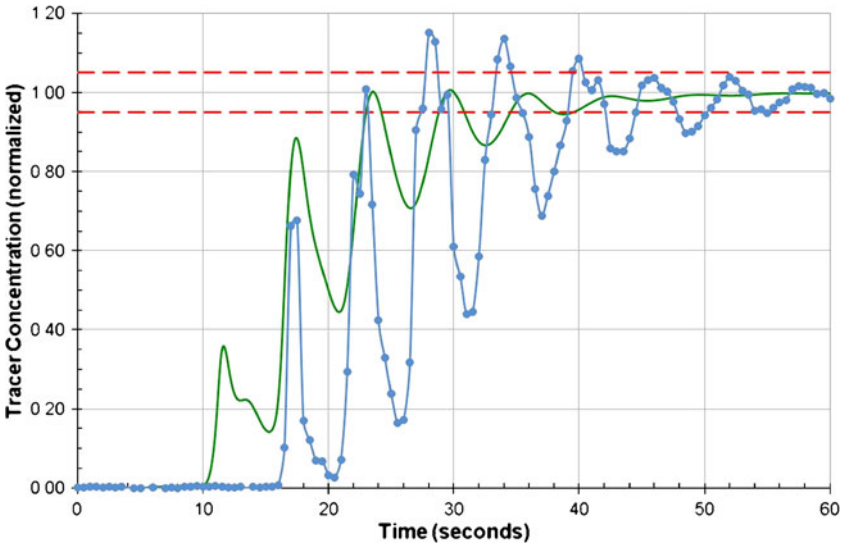

Fig. 2. Methylparaben concentration *vs* time for commercial-scale tank at 45 rpm and 2,500 l fill volume. Experimental (*circles*) and CFD simulation (*solid line*)

upon addition of the tracer to the tank (analogous to methylparaben in experiment) to the tank. Blend time is defined as the time needed to reach 95% of the final concentration and is independent of the final concentration reached. Blend time only depends on the type of impeller, geometry of the tank, liquid volume and the stirrer speed. Blend time does not depend on the type of tracer used, initial concentration of the tracer aliquot or the final concentration of the tracer. Hence it was not required to maintain the final tracer concentration same for the experiments and for the CFD simulation. In order to be able to compare the experimental and CFD simulation results, the tracer concentrations were normalized to the respective final, mean concentrations. A comparison between the model predictions and experimental data was a simple confirmation of the CFD model to simulate the actual flow field in the tank. Experimental conditions for the blend time studies are listed in Table IV.

RESULTS AND DISCUSSION

Experimental measurements of liquid–liquid blend time and corresponding CFD simulations were conducted in the commercial-scale tank at impeller speeds of 45 and 75 rpm. Figures 2 and 3 show profiles of methylparaben concentration as a function of time for each impeller speed studied. The concentration data in both figures have been normalized to the final, mean concentration.

For both impeller speeds, similar transient behavior is seen between the experimental measurements and the CFD simulations. The methylparaben tracer disperses throughout the tank in a series of damped out concentration waves when viewed from a fixed reference point. For the 45 rpm case, the period of one complete oscillation is approximately 5.7 s for the experimental measurements and 6.0 s for the CFD simulations (see Figs. 2 and 3). This is indicative of the tank's overall circulation or turnover time. Similarly, the period of

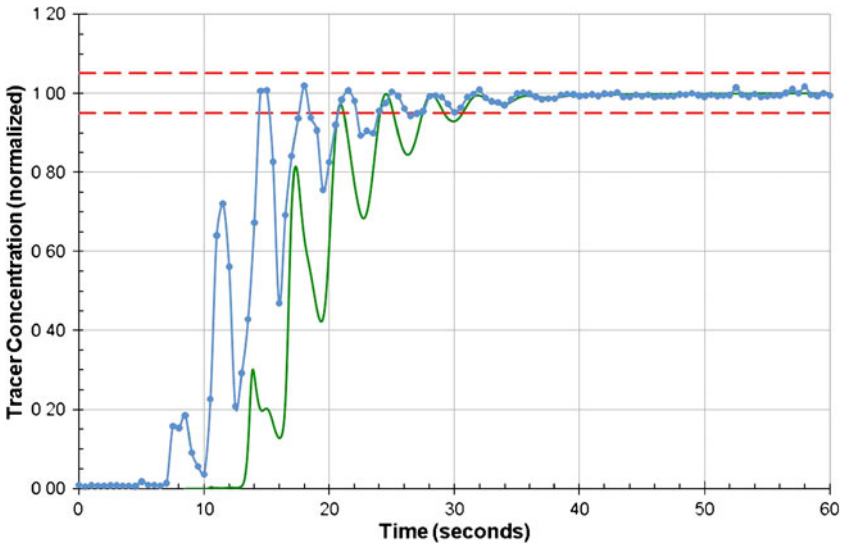

Fig. 3. Methylparaben concentration *vs* time for commercial-scale tank at 75 rpm and 2,500 l fill volume. Experimental (*circles*) and CFD simulation (*solid line*)

Table V. Blend Time (Θ_{95}) for Experimental Measurements and CFD Simulations on Commercial-Scale Tank at 2,500 l Fill Volume

	Θ_{95} (s)	
Impeller Speed (rpm)	Experimental	CFD Simulation
45	55	38
75	27	22

CFD computational fluid dynamic

oscillation for the 75 rpm case is approximately 3.3 s for the experimental measurements and 3.4 s for the CFD simulations. In all cases, blending to within 5% of the mean is achieved after approximately five to six tank turnovers. Table V below lists blend time (Θ_{95}) values. In both cases, the blend times as predicted by CFD are slightly shorter than the measurements. It was also seen that the experimental blend time was more sensitive to stirrer speed as compared with the predicted blend time from CFD simulation. Experiments showed ~50% decrease in blend time when stirrer speed was changed from 45 to 75 rpm as opposed to ~40% decrease seen for CFD simulations. These results provide reasonable confidence in the CFD simulations to predict the flow field in the commercial-scale tank. Since only two data points are available, no statistical tests will provide meaningful results.

A set of ten experiments were conducted at laboratory and commercial scale. Propylparaben dissolution was monitored using UV/Vis spectroscopy. Mixing speeds were scaled up from lab scale to commercial scale to maintain similar P/V at both scales as determined by CFD modeling. Comparisons of the dissolution profiles for sample of three experiments are shown in Figs. 4, 5, and 6. We can see that the dissolution profiles at lab and commercial scales are in reasonable agreement with each other. One metric that is used to quantify dissolution time is the time for 90% dissolution, t90. This information is tabulated in Table VI for all the experiments conducted at lab and commercial scale. The simple scale-up principle of P/V has resulted in good prediction of t90 at commercial scale from lab-scale experiments. The discrepancy between t90 values and the overlay of dissolution profiles at slower mixing speeds can be explained by the observation that propylparaben formed agglomerated lumps immediately upon addition to commercial-scale tank. These lumps eventually dispersed for complete dissolution. One improvement in the CFD model could be to take into consideration turbulent energy dissipation rates at the length scales of the agglomerated particle sizes to account for differences in particle agglomeration behavior at the two scales. In spite of the above shortcomings in the accuracy of prediction, we think the lab-scale mixing studies that are scaled up using a simple CFD modeling approach involving determination of P/V, sufficiently describes the mixing phenomena at commercial scale. The final concentrations of the solution in the mixing tanks are confirmed with HPLC analysis.

A simple linear regression between t90 values observed at lab scale and commercial scale provided a 90% confidence interval for the slope as 0.8–1.5. This suggests that there is no evidence to reject the null hypothesis (slope is 1). A slope of 1 indicates perfect correlation between the t90 values observed

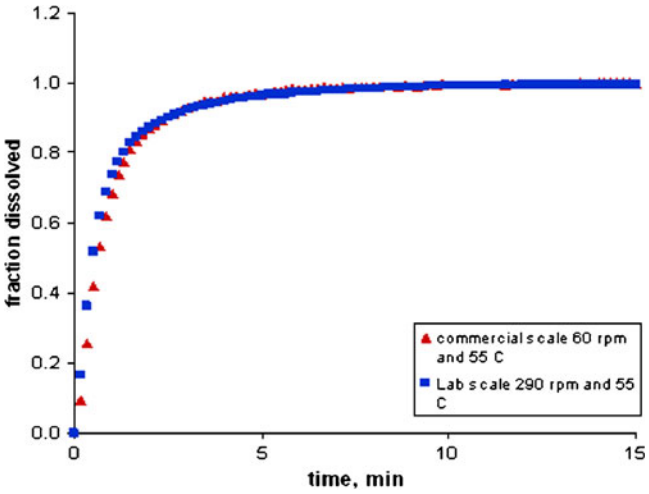

Fig. 5. Comparison of lab-scale and commercial-scale dissolution profiles for run ID #5

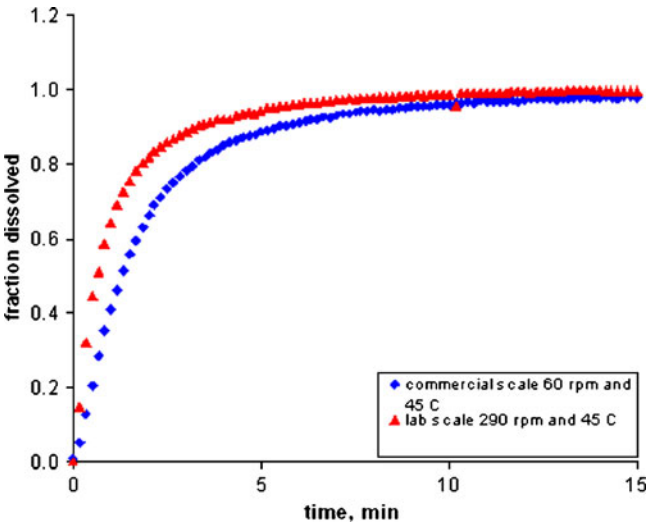

Fig. 4. Comparison of lab-scale and commercial-scale dissolution profiles for run ID #2

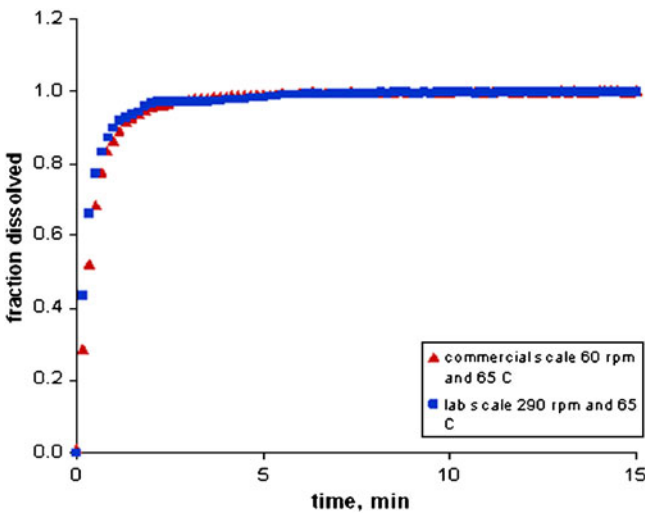

Fig. 6. Comparison of lab-scale and commercial-scale dissolution profiles for Run ID #9

Table VI. Comparison of Time for 90% Dissolution Between Lab and Commercial-Scale Runs

Run ID	Mixing Speed at Lab Scale (rpm)	Mixing Speed at Commercial Scale (rpm)	Operating Temperature (°C)	Time for 90% Dissolution at Lab Scale, t90—Lab (min)	Time for 90% Dissolution at Commercial Scale, t90—Commercial (min)
1	210	45	45	6.00	7.16
2	290	60	45	3.33	5.63
3	360	75	45	2.33	4.1
4	210	45	55	1.67	3.83
5	290	60	55	2.47	2.53
6	290	60	55	2.48	2.59
7	360	75	55	1.17	2.17
8	210	45	65	1.33	1.9
9	290	60	65	1.00	1.38
10	360	75	65	0.83	1.13

A simple linear regression between t90 at lab and commercial scales gives a 90% confidence interval of slope as 0.8–1.49

at the two scales. This simple correlation is not useful to use the regressed model as the prediction of t90 values at commercials scale. A rigorous statistical analysis follows to predict the t90 at commercial scale from lab-scale experiments, when the commercial-scale mixing speeds are selected based on the equal P/V between lab and commercial scales.

Statistical analysis was conducted utilizing the dissolved fraction (p) values from the ten experiments. The goal of this analysis is to answer one simple question: If we observe a t90 at lab scale, what will be the expected value of t90 at commercial scale if the mixing conditions were scaled based on similarity of P/V between the two scales? To answer this question, the fraction of propylparaben dissolved, p, was transformed into logit (p) defined as follows;

$$\text{logit}(p) = \ln\left(\frac{p}{1-p}\right) \tag{9}$$

Logit is a variance stabilizing transformation which allows combining continuous variable like time and categorical variables like scale (lab or commercial) into one equation. This transformation of the data results in Fig. 7 where the logit (p) is plotted as a function time for each of the experimental run at two scales. Averaging over ten experimental runs at a given time point we arrive at the following relationship between logit (p) and dissolution time and scale of operation:

$$\begin{aligned} &\text{logit}(p) = \ln\left(\tfrac{p}{1-p}\right) \\ &= 0.6005 - 0.6534I(\text{comm}) \\ &+0.7627\text{Time} \\ &= f(\text{scale}, \text{Time}) \\ &\Rightarrow p = \tfrac{1}{1+e^{-f(\text{scale},\text{Time})}} \end{aligned} \tag{10}$$

Where I=1 for commercial scale and 0 for lab scale.

The above relationship can further be simplified as follows to demonstrate scalability of conditions between lab and commercial scale at any given time:

$$\begin{aligned} &\ln\left(\tfrac{p_c}{1-p_c}\right) - \ln\left(\tfrac{p_L}{1-p_L}\right) = -0.6534(\pm 0.4425) \\ &\Rightarrow p_c = \tfrac{\frac{p_L}{1-p_L}}{\frac{p_L}{1-p_L}+e^{0.6534}} \end{aligned} \tag{11}$$

Where p_c is the fraction dissolved at commercial scale and p_L is the fraction dissolved at lab scale. A practical application of the above relationship is described as follows—if 90% of solids are dissolved in lab scale in a given time (t90), then substituting p_L=0.9 in the above relation we arrive at p_c (fraction dissolved at commercial scale)=0.824 with a 95% confidence interval of 0.75–0.88 at the same time t90. The above analysis which is an average of ten experiments in lab and commercial scale provides a way to scale-up the mixing speeds to commercial scale based on the equality of P/V at the two scales. This simple technique provides sufficiently accurate predictions of dissolution behavior at commercial scale.

CONCLUSIONS

In this work, we have successfully demonstrated that scale-up of solid dissolution can be achieved using a systematic process of lab-scale experiments followed by simple CFD modeling to predict commercial-scale experimental conditions. In particular this method is sought to identify major dissolution issues at lab scale before the large expenses of processing and raw materials (particularly API) are committed.

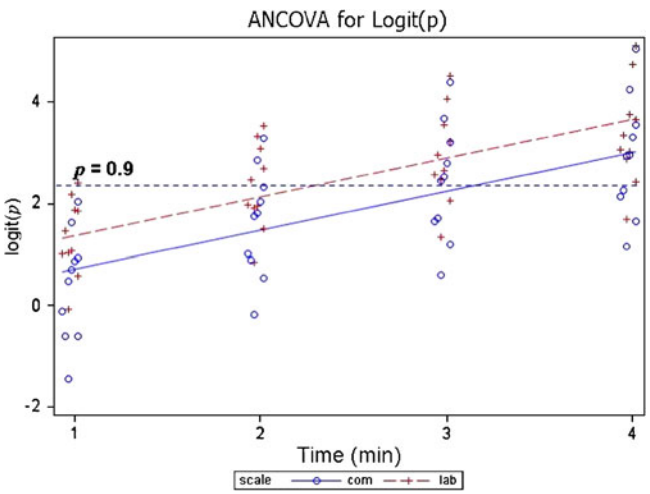

Fig. 7. Analysis of covariance between lab and commercial-scale logit (p)

The results show good prediction of commercial-scale dissolution profiles from lab-scale experiments. Utilizing statistical analysis, we have been able to predict that a time (t90) that corresponds to 90% dissolution at lab scale will correspond to 82.4% dissolution at commercial scale with a 95% confidence interval between 75–88% when the mixing speeds are scaled up based on equality of P/V at the two scales. This practical method of data analysis shows that the simple approach of scaling up liquid mixing based on similarity of P/V at the two scales provides a good prediction of liquid mixing and dissolution at commercial scale based on lab-scale experiments. This approach paves a way to utilize modeling in scaling up liquid mixing processes towards the direction of quality by design.

REFERENCES

1. Brian PLT, Hales HB, Sherwood TK. Transport of heat and mass between liquids and spherical particles in an agitated tank. AIChE J. 1969;15:727–33.
2. Levins DM, Glastonbury JR. Application of Kolmogorofff's theory to particle–liquid mass transfer in agitated vessels. Chem Eng Sci. 1972;27:537–43.
3. Levins DM, Glastonbury JR. Particle-liquid hydrodynamics and mass transfer in a stirred vessel. 2. Mass transfer. Trans Inst Chem Eng. 1972;50:132–46.
4. Okamoto Y, Nishikawa M, Hashimoto K. Energy Dissipation rate distribution in mixinig vessels and its effects on liquid–liquid dispersion and solid-liquid mass transfer. Int Chem Eng. 1981;21: 88–91.
5. Kresta SM, Paul EL. Handbook of Industrial Mixing: Science and Practice. New York: Wiley; 2003.
6. Pangarkar VG, Yawalkar AA, Sharma MM, Beenackers AACM. Particle–liquid mass transfer coefficient in two-/three-phase stirred tank reactors. Ind Eng Chem Res. 2002;41:4141–67.
7. Perry RH, Green DW. Perry's Chemical Engineers' Handbook. New York: McGrawHill; 2008.
8. Barker JJ, Treybal RE. Mass-transfer coefficients for solids suspended in agitated liquids. AIChE J. 1960;6:289–95.
9. Hughmark GA. Hydrodynamics and mass transfer for suspended solid particles in a turbulent liquid. AIChE J. 1974;20:202–4.
10. Yu Lawrence X. X. Pharmaceutical quality by design: product and process development, understanding, and control. Pharm Res. 2008;25:781–91.
11. Ranade VV. Computational flow modeling for chemical reactor engineering. San Diego, CA: Academic Press; 2002.
12. Yeoh SL, Papadakis G, Yianneskis M. Numerical simulation of turbulent flow characteristics in a stirred vessel using the LES and RANS approaches with the sliding/deforming mesh methodology. Chem Eng Res Des. 2004;82:834–48.
13. Rielly CD, Habib M, Sherlock JP. Flow and mixing characteristics of a retreat curve impeller in a conical-based vessel. Chem Eng Res Des. 2007;85:953–62.
14. Jaworski Z, Bujalski W, Otomo N, Nienow AW. CFD study of homogenization with dual Rushton turbines. Comparison with experimental results. Part I: initial studies. Chem Eng Res Des. 2000;78:327–33.
15. Grant DJW, Mehdizadeh M, Chow AHL, Fairbrother JE. Non-linear van't Hoff solubility-temperature plots and their pharmaceutical interpretation. Int J Pharm. 1984;18:25–38.